Pairing strength and proton characters of the N7,N9-dimethylated GC and AT base pairs: a density functional theory investigation†

Dianxiang Xing,[ab] Xiaohua Chen[a] and Yuxiang Bu*[a]

Received (in Montpellier, France) 20th February 2007, Accepted 4th May 2007
First published as an Advance Article on the web 29th May 2007
DOI: 10.1039/b702640d

The pairing strength, proton properties associated with proton transfer and deprotonation as well as relevant structural perturbations of 7,9-dimethyl GC ($[mGC]^+$) and 7,9-dimethyl AT ($[mAT]^+$) base pairs have been investigated. Energies related to proton transfer and deprotonation have also been predicted. It is found that the guanine/adenine N7 methylation improves the stability of GC/AT base pair. The proton transfer between the guanine N1 and the cytosine N3 is observed in $[mGC]^+$ with an out-of-plane transition state. However, no proton-transfer reaction occurs for $[mAT]^+$. For the deprotonation of $[mGC]^+$ and $[mAT]^+$, guanine C8 and N1 and adenine C8 are the most favorable sites. Deprotonation from the pyrimidine N1 site generates the most stable deprotonated base pairs, and the dissociation energies surprisingly amount to $\sim$100.00 and $\sim$65.49 kcal mol^{-1}, respectively, much higher than those of their neutral base pairs. Deprotonation from the other sites of pyrimidine exhibits the most significant structural changes and gives the most interesting deprotonated base pairs. This process is accompanied by a barrier-free proton transfer (BFPT) from guanine N1 to cytosine N3 or adenine N6 to thymine N3 or O4 site. In this way, two rare imino tautomers of cytosine (*trans*-C* or *cis*-C*) are easily generated by removing a proton from the N4 site of cytosine in $[mGC]^+$. In addition, the reason for BFPT from guanine N1 to cytosine N3 has been explored.

1 Introduction

Acidity and basicity properties of nucleic bases and their derivatives are essential for understanding many mechanisms of fundamental importance in biological processes.[1] Proton acceptor and/or proton donor abilities modulate the hydrogen bonding capacity of DNA and RNA bases, and the interaction energy between two bonded complementary bases depends on the intrinsic basicity of the acceptor atoms as well as on the acidity of donor hydrogen. The gas-phase acidity (GPA) is usually the major thermodynamic parameter available for a quantitative understanding of the intrinsic properties in the absence of solvents. In recent years, studies on, proton-transfer processes, the protonation and deprotonation processes for various systems have become popular subjects.[2–10] Experimentally, the ionized compounds can be easily obtained using various methods,[3] such as chemical ionization, fast atom bombardment ionization, electrospray ionization, or matrix-assisted laser desorption ionization. The GPAs can be determined employing the most-used three methods, that is, equilibration measurements, reaction bracketing, and kinetic methods. However, there are some limitations when treating some systems that have intramolecular H-bonds or possess several possible sites for deprotonation, despite their merits.[3] For common biological systems containing more active sites, it is difficult to measure the GPAs for the less active sites experimentally since experiment can only give the GPAs for the most active sites.[2] Moreover, geometries or structural changes for the systems investigated are still difficult to obtain. On the other hand, theoretical calculations based on various theories and methods have been proven to be a useful tool to explore deprotonation processes since they are capable of providing information about all possible sites of deprotonation within a given molecule on an equal footing.[10d] What is more, the applications of theoretical calculations are important for those chemical systems that are not amenable to experiments.

It is well known that the N7 position of guanine in double-stranded DNA and single-stranded DNA or RNA is readily accessible to chemical attack and therefore a preferred target for alkylating agents or metal ions.[11–13] Methyl carbonium, which is derived from methane diazonium ion, preferentially covalently binds to this site and 7-methylguaninium has often been thought to be a mono-cation complex.[14–16] The exogenous methylation of the more electronegative sites in the nucleoside acid bases such as N7, N3 and O6 in the purines and O2, O4 and N3 in the pyrimidines is also known to be responsible for mutagenic events.[17–19] Additionally, covalent binding of methyl to guanine can strongly affect the electron distribution in the bases and thus also the acidity and base pairing. Prior theoretical research shows that 7-methylation may enhance the guanine base-pairing strength by *ca.* 10 kcal mol^{-1}, and it also causes a *ca.* 90 kcal mol^{-1} drop of the

[a] *Institute of Theoretical Chemistry, Shandong University, Jinan, 250100, P. R. China. E-mail: byx@sdu.edu.cn*
[b] *School of Chemical Engineering, Shandong Institute of Light Industry, Jinan, 250353, P. R. China*

† Electronic supplementary information (ESI) available: Geometric characteristics of all species derived from GC/$[mGC]^+$ (Table S1) and AT/$[mAT]^+$ (Table S2). See DOI: 10.1039/b702640d

deprotonation energy of guanine H1.[16] On the other hand, experimental results reveal that 7-methylguaninium cation has a low pK_a of *ca.* 7,[20] while N7-platinated guanine has a slightly higher pK_a of *ca.* 8.[11]

Adenine methylation has been suggested to be as important as guanine methylation.[21] The N3 site of adenine is thought to be the second most favored site of methylation, second to the N7 site of guanine.[22] Aside from the N3 site of adenine, covalent binding of methylation to adenine N7 site was also observed.[23] Similar enhanced acidification and pairing stabilities should be expected for N7-methyladeninium. In purine–pyrimidine base pairs, the enhanced acidification of purine will increase the possibility of deprotonation or proton transfer between bases and thus greatly change the proton characters of interacting bases through polarization. Previous studies have mainly centered on mutagenesis,[24] tautomerization of N7-methylation purine[25] and the reactivity of methane diazonium ions with purine.[26] Also, a number of theoretical studies have focused on the effect of metal ions on the H-bond strength of base pairs and proton transfer in base pairs[27–32] or the H-bond strength between the natural bases.[33] Yet few researches have specially concerned the influence of guanine/adenine N7 methylation on the strength of Watson–Crick base pairing and acid–base properties of GC/AT base pairs.

In the present study, we report our theoretical study about the effect of guanine/adenine N7 methylation on base pairing strength and acid–base properties associated with proton transfer and deprotonation of GC and AT pairs. The geometrical changes during deprotonation and the dissociation energies of the deprotonated structures are also analyzed. In this work, deoxyribose fragments bonded to the N9 sites of guanine and adenine in DNA are modeled as methyl, since alkylation at the N9 position of guanine hardly affects the electronic structure or acidity of the base and base pairing strength.[16] That is, the pairing strength of N7,N9-dimethylguaninium-cytosine ($[mGC]^+$) and N7,N9-dimethyladeninium-thymine ($[mAT]^+$) and acid–base properties of $[mGC]^+$ and $[mAT]^+$ were investigated.

2 Computational details

Molecular geometries and harmonic vibrational frequencies of the considered structures have been obtained by using the nonlocal hybrid three-parameter density functional approach[34,35] as implemented in the Gaussian 98 program.[36] The B3LYP method is used in this work along with the basis set of 6-31+G* because it shows good accuracy[37–39] with comparatively low cost in computational time. Final energy evaluation has been performed at B3LYP/6-311++G**//B3LYP/6-31+G* level.

The gas-phase acidity (GPA) for the following deprotonation process, $HB \rightarrow H^+ + B^-$, is calculated as GPA = $E(H^+)$ + $E(B^-)$ − $E(HB)$, in which $E(i)$ refers to the total electronic energy of the species *i*. This equation applies also to the systems $[HB]^+ \rightarrow H^+ + B$. For the protonation process, $H^+ + B \rightarrow HB^+$, the corresponding proton affinity (PA) can be also calculated according to the equation PA = $E(HB^+)$ − $E(H^+)$ − $E(B)$. It is a good way to predict the acidity or basicity for the different active sites qualitatively employing the calculated GPA or PA. For the deprotonation processes, the larger the value of GPA is, the weaker the acidity is, while for the protonation processes, the larger the PA is, the stronger the basicity is.

The dissociation energy (D_e) of a pair is defined as the difference between the total energy of the base pair and the sum of the total energies of the individual moieties. At the same time, the dissociation energy has been corrected for the basis set superposition error (BSSE) using the Boys–Bernardi counterpoise (CP) scheme.[40] The predicted dissociation energies for all structures considered can also be regarded as interaction or stabilization or hydrogen bonding energy of the base pair. Obviously, the larger the dissociation energy is, the more difficult to dissociate into its component bases the base pair is.

To elucidate the intermolecular H-bonds interaction, natural bond orbital (NBO) and charge distribution are further analyzed at B3LYP/6-311++G** level with B3LYP/6-31+G* geometry. Since the occupancies of the filled NBOs are highly condensed, the delocalizing interactions can be treated by the second-perturbation energies $E(2)$

$$E(2) = \Delta E_{ij} = n_i \frac{(F_{ij})^2}{\varepsilon_j - \varepsilon_i}$$

where $F(i, j)$ is the off-diagonal NBO Fock matrix element describing the donor–acceptor interaction and n_i is the donor orbital occupancy, ε_i, ε_j are diagonal elements (orbital energies).[41]

All computations are performed for the gas-phase structures without considering solvent effects, because the influence of the surrounding is likely to be energetically small for proton transfer between hydrogen-bonded stacked DNA bases in duplex DNA.[42] Within the DNA stacked bases, the solvent is excluded, and the DNA interior has a relatively low dielectric constant.[43]

The atomic numbering of N7,N9-dimethylated guaninium-cytosine ($[mGC]^+$) and N7,N9-dimethylated adeninium-thymine ($[mAT]^+$) base pairs are displayed in Fig. 1. The notation used to denote the deprotonated structure is as follows: the proton is removed from $[mGC]^+$ or $[mAT]^+$ at the site mentioned in parentheses, forming the base preceding the parentheses. For example, the deprotonated mG(C8)C is generated by the removal of a proton from the C8 site of mG^+. Sometimes, for simplification, mG($-H^+$)C/mG($-H^+$) or mGC($-H^+$)/C($-H^+$) is generally used to denote deprotonation from sites on mG^+ or cytosine. To investigate the effect of deprotonation on the geometry of the deprotonated structure, two dihedral angles were considered:

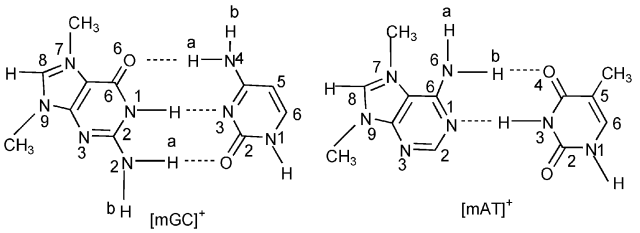

Fig. 1 Atomic numbering of $[mGC]^+$ and $[mAT]^+$ base pairs.

Table 1 Selected geometrical parameters of $[mGC]^+$, $[mGC]^+_{TS}$, $[mGC]^+_{PT}$, $[mAT]^+$ and the neutral GC and AT systems[a]

	O6–H4a	O6–N4	N1–H	N3–H1	N1–N3	O2–H2a	O2–N2	D1[b]	D2[b]
GC	1.789	2.825	1.033	1.934	2.967	1.920	2.943	0.0	0.0
$[mGC]^+$	1.941	2.960	1.048	1.868	2.915	1.767	2.801	0.0	0.0
$[mGC]^+_{TS}$	1.660	2.700	1.382	1.273	2.654	1.789	2.805	−10.7	−6.6
$[mGC]^+_{PT}$	1.619	2.672	1.776	1.069	2.841	1.971	2.980	0.0	0.0

	O4–H	O4–H–N6	N1–H	N1–H–N3	D1[c]	D2[c]
AT	1.927	174.2	1.870	178.7	−0.0	0.0
$[mAT]^+$	1.763	178.8	1.993	174.5	−0.1	0.0

[a] Distances in Å, angles in degrees. [b] D1 and D2 denote the dihedral angles G(O6–C2)–C(C2–C4) and G(C6–N1)–C(N3–C4), respectively. [c] D1 and D2 denote the dihedral angles A(C6–N1)–T(N3–C4) and A(N1–C2)–T(C2–N3), respectively.

G(O6–C2)–C(C2–C4) and G(C6–N1)–C(N3–C4) angles for $[mGC]^+$, as well as A(C6–N1)–T(N3–C4) and A(N1–C2)–T(C2–N3) angles for $[mAT]^+$.

3 Results and discussion

3.1 The pairing of $[mGC]^+$ and $[mAT]^+$ base pairs

3.1.1 Structures and the pairing strength of $[mGC]^+$ and $[mAT]^+$. After methylation, guanine should become more acidic, and thus those H-bonds in which guanine acts as proton donors are strengthened, however, those in which guanine acts as proton acceptors are weakened in comparison with its neutral species (*e.g.* without methylated GC pair). As expected, the N3···H1 and O2···H2a H-bond in which guanine acts as a proton donor are shortened, while the O6···H4a bond in which guanine acts as a proton acceptor is lengthened, Table 1 (the atomic numbering shown in Fig. 1). Such changes follow the same trends as the metal ions modified GC and GC cation.[31,32] The situation for $[mAT]^+$ base pair is very similar. The H6a···O4 H-bond in which purine acts as a proton donor decreases by 0.164 Å compared with the neutral AT, while N1···H3 in which this monomer acts as proton acceptor increases by 0.123 Å. For the proton-transferred structure $[mGC]^+_{PT}$, it can also be predicted that cytosine becomes more acidic after proton transfer, and thereby N1···H–N3 and O6···H4a in which cytosine acts as proton donors are shortened, and that O2···H2a in which cytosine acts as proton acceptor is lengthened with respect to the neutral GC base pairs. Also, the H-bond distances are changed as predicted (Table 1). In addition, all of the three base pairs still remain planar.

Quantitatively, the dissociation energies should reflect the changes of the H-bond distances for the three base pairs. Table 2 shows that the GC base pair becomes ~10 kcal mol^{-1} more stable after methylation (34.14 *vs.* 24.67 kcal mol^{-1}). Actually, the same result has also been obtained by Burda *et al.* employing MP2/6-31G*,[16] which also verifies that our basis sets are enough for the final energy evaluation. Similarly, methylation provides ~4 kcal mol^{-1} more pairing energy for $[mAT]^+$ base pair, (16.06 for $[mAT]^+$ *vs.* 11.96 kcal mol^{-1} for AT pair). For the proton-transferred structure $[mGC]^+_{PT}$, the dissociation energy is greatly increased by ~28.0 kcal mol^{-1}. In addition, the BSSEs are also employed to correct the basis set superposition error. As listed in Table 2, the BSSEs produced in the calculations of the dissociation energies are less than 1.2 kcal mol^{-1}, a relatively small quantity, further implying that the 6-311++G** adopted in this work should be an appropriate basis set. Here, the dissociation schemes of dimethylation GC and AT base pairs are as follow: $[mGC]^+$ is dissociated into mG^+ and the neutral cytosine, $[mGC]^+_{PT}$ is dissociated into mG(N1) and cytosine($+H^+$) cation, while $[mAT]^+$ is dissociated into mA^+ and the neutral thymine.

3.1.2 NAO charge distribution and NBO analysis. To analyze the nature of H-bond strength, electronic structures of the three base pairs have been explored. NAO charges for $[mGC]^+$/$[mAT]^+$ show that the charge on mG^+ and mA^+ moiety amounts to 0.914 and 0.977 e, respectively, Table 3. The positive charge is distributed over the whole guanine/adenine fairly proportionally, decreasing the negative charges (absolute value) and increasing the positive charges of individual atoms on guanine/adenine. This leads to H-bonds involving H1 and H2a of guanine strengthened and the H-bond involving O6 of guanine weakened. For $[mAT]^+$, the redistribution of the charge on adenine enhances the strength of N6–H6a···O4 bond and weakens the strength of N1···H3–N3 bond, which are consistent with the changes of the H-bond distances as mentioned above. The situation for $[mGC]^+_{PT}$ is very similar, 0.835 e is located on cytosine (Table 3), also, the positive charge on cytosine increases the positive charges and decreases the negative partial charges of individual atoms. In addition, after the proton transfer, the guanine O6 and N1 atoms gain more negative charge than those in $[mGC]^+$, while the cytosine N2 atom gains a small negative charge. Thus, the

Table 2 The dissociation energies of the GC, AT and $[mGC]^+$, $[mGC]^+_{PT}$, $[mGC]^+_{TS}$ and $[mAT]^+$ base pairs (energies in kcal mol^{-1})[a]

GC[b]	$[mGC]^+$ [a]	$[mGC]^+_{PT}$	$[mGC]^+_{TS}$	AT	$[mAT]^+$
25.63	34.71	53.73	53.73	12.68	16.85
24.67	34.14	52.59	52.59	11.96	16.06

[a] The data in the first row are referred to those calculated without the BSSE correction, while the data in the second row are referred to those calculated with the BSSE correction. [b] MP2 results for GC and AT base pairs are 26.30 and 12.30 kcal mol^{-1}, respectively (with BSSE correction), taken from ref. 32*b*. [c]MP2 results for $[mGC]^+$ are 41.66 (without BSSE correction) and 35.89 kcal mol^{-1} (with BSSE correction), taken from ref. 16.

Table 3 NBO partial charges on selected atoms of $[mGC]^+$, $[mGC]^+_{PT}$, $[mAT]^+$ and the neutral GC and AT base pairs as well as total charges on the isolated bases

	H1(G)	H2a	O6	N1	mG[a]	Gua[b]	O2(C)	N3	H4a	Cyt[c]
GC	0.447	0.437	−0.681	−0.645		−0.025	−0.688	−0.655	0.450	0.025
$[mGC]^+$	0.463	0.469	0.650	−0.637	0.914	0.265	−0.693	−0.667	0.437	0.086
$[mGC]^+_{PT}$	0.469	0.426	−0.730	−0.686	0.165	−0.465	−0.615	−0.628	0.454	0.835

	N1(A)	H6a	mA[a]	Ade[b]	O2(T)	H3	O4	Thy[c]
AT	−0.620	0.435		0.027	−0.633	0.462	−0.655	−0.027
$[mAT]^+$	−0.567	0.456	0.977	0.328	−0.624	0.447	−0.675	0.024

[a] The total charges on mA or mG moiety. [b] The total charges on adenine or guanine moiety. [c] The total charges on cytosine or thymine in respective base pair.

H-bond O6···H4a–N4 and N1···H–N3 is shortened, but N2–H2a···O2 is lengthened.

Of course, the nature of H-bonds could also be understood on the basis of the donor–acceptor orbital interaction. As can be seen from Table 4, the interactions from guanine O6 lone pairs (LPs) to cytosine σ^*_{N4-H4a} decrease by 10.88 kcal mol^{-1} totally, while the total interactions from cytosine N3 lone pair (LP) to guanine σ^*_{N1-H1} and O2 LPs to guanine σ^*_{N2-H2a} increase by 15.98 kcal mol^{-1} with respect to those of the neutral GC, indicating that the N1···H–N3 and N2–H2a···O2 bonds are strengthened, while the O6···H4a–N4 bond is weakened. This reinforces our earlier conclusion about the strength of the three H-bonds. On the other hand, from the H-bond orbital interactions, it can be deduced that N3···H1–N1 and N2–H2a···O2 are the significant contributions to the stability of $[mGC]^+$. But for $[mGC]^+_{PT}$, the sum of interactions from guanine O6 LPs to cytosine σ^*_{N4-H4a} are enhanced by 20.01 kcal mol^{-1}, the interaction from guanine N1 LP to σ^*_{N3-H3} increases by 16.92 kcal mol^{-1}, with respect to those of the neutral GC. While those from cytosine O2 LPs to guanine σ^*_{N2-H2a} are totally reduced by 3.35 kcal mol^{-1}, indicating that the proton transfer makes O6···H4a–N4 and N1···H–N3 strengthen and O6···H2a–N2 weaken. Moreover, all of these orbital interactions suggest that the contributions to the stability of $[mGC]^+_{PT}$ mainly originate from the O6···H4a–N4 and N1···H–N3 H-bonds, especially the former. In the case of $[mAT]^+$, as anticipated, the increase of the interaction energies from thymine O2 LPs to adenine σ^*_{N6-H6a} sums up to 11.77 kcal mol^{-1} (Table 4), while those from adenine N1 LPs to thymine σ^*_{N3-H3} totally decreases by 9.48 kcal mol^{-1} with respect to those of AT. Also, the N6–H6a···O4 bond is the only origin of the stability of $[mAT]^+$ base pair.

3.2 Proton transfer between bases of $[mGC]^+$ and $[mAT]^+$

As mentioned above, H1 and H2a in mG^+ become more positive. Thus, any or both of the two protons can be involved in single or double proton-transfer reaction. However, only single proton-transfer from mG^+ N1 to cytosine N3 is obtained, but the proton transfer from guanine N2 to O2 of cytosine is not observed. This was somewhat unexpected because the gas-phase proton affinities of O2 and N3 sites of cytosine differ by less than 1 kcal mol^{-1}.[9] Moreover, O2-protonated cytidine monophosphate has been observed in acidic aqueous solution.[10a] The reason that proton H2a does not transfer to O2 of cytosine seems to reside in the larger energy requirement for deprotonation from the N2 site than N1 site of guanine. This will be discussed in Section 3.3.2.

During the proton-transfer process of $[mGC]^+$, two bases gradually come close to each other and then form the transition state. At the transition state, the upper two H-bonds O6–N4 and N1–N3 are shortened from 2.960 and 2.915 to 2.700 Å and 2.655 Å, respectively, while O2–N2 is slightly

Table 4 Primary delocalization interaction energies occurring between the orbitals in unit 1 and 2 of base pairs GC, $[mGC]^+$, $[mGC]^+_{PT}$, AT and $[mAT]^+$ (in kcal mol^{-1})[a]

	1 → 2[b]			2 → 1		
	$n1_{O6} \rightarrow \sigma^*_{N4-H4a}$[c]	$n2_{O6} \rightarrow \sigma^*_{N4-H4a}$[c]	$n_{N1} \rightarrow \sigma^*_{N3-H3}$	$n_{N3} \rightarrow \sigma^*_{N1-H1}$	$n1_{O2} \rightarrow \sigma^*_{N2-H2a}$	$n2_{O2} \rightarrow \sigma^*_{N2-H2a}$
GC	7.02	14.75	(—)	18.04	3.80	8.61 (52.22)
$[mGC]^+$	4.16	6.73	(—)	24.07	7.02	15.34 (57.32)
$[mGC]^+_{PT}$	8.66	33.12	34.96	(—)	3.43	5.63 (85.80)

	1 → 2[b]		2 → 1
	$n1_{O4} \rightarrow \sigma^*_{N6-H6a}$	$n2_{O4} \rightarrow \sigma^*_{N6-H6a}$	$n_{N1} \rightarrow \sigma^*_{N3-H3}$
AT	4.27	7.44	22.58 (34.29)
$[mAT]^+$	7.14	16.34	13.10 (36.58)

[a] Unit 1 and Unit 2 denote mG^+ moiety and cytosine moiety, respectively, in GC system. [b] Unit 1 and Unit 2 denote thymine and mA^+, respectively, in AT system. [c] $n1_O \rightarrow \sigma^*_{N-H}$ and $n2_O \rightarrow \sigma^*_{N-H}$ stand for the interactions of two lone pairs of oxygen atom with N–H antibonding orbital. A dash (–) indicates that the structure has no delocalization interaction between these two orbitals. Values in parentheses denote the sum of all delocalization interaction energies.

Table 5 The activation energies (kcal mol^{-1}) of proton transfer[a,b]

	$[mGC]^+$	$[mGC]^+_{PT}$	E_a^{+} [c]	E_a^{-} [d]
*E*1	0	6.01	6.93	0.92
*E*2	0	5.45	3.83	−1.61

[a] $[mGC]^+_{PT}$ is relative to $[mGC]^+$; the forward and reverse activation energies of $[mGC]^+_{TS}$ are relative to $[mGC]^+$ and $[mGC]^+_{PT}$, respectively. [b] *E*2 is referred to the energies with zero-point vibration correction. [c] E_a^{+} is the forward activation energy. [d] E_a^{-} is the reverse activation energy.

lengthened. Similar changes have been observed in previous theoretical study on the proton transfer of GC^+ and the metal cation modified GC base pair.[29,31] A slight out-of-plane rocking of the pair during the proton-transfer process is also predicted. It must be mentioned that the stable geometries of the $[mGC]^+$ and $[mGC]^+_{PT}$ are planar, but the geometry of the transition state is not in plane. The G(C6–N1)–C(N3–O4) is −10.7° and G(N1–C2)–C(O2–N3) is −6.6°.

Table 5 shows that the transfer of H1 from guanine to cytosine is endothermic by 6.01 kcal mol^{-1}. The forward activation energy for the proton transfer of the $[mGC]^+$ cation is 6.93 kcal mol^{-1}, while the reverse activation energy is only 0.92 kcal mol^{-1}. However, if taking the correction of the zero-point vibration energy into consideration, the forward activation energy decreases to 3.83 kcal mol^{-1}. At the same time, the reverse activation energy decreases to −1.61 kcal mol^{-1}. This implies that the reverse process is spontaneous and fast. So the formation of $[mGC]^+_{PT}$ would be scarcely observed in the gas-phase. Even in the water solvent, the formation of the proton-transferred structure is unfavorable, since the dipole moment of $[mGC]^+_{PT}$ is smaller than that of $[mGC]^+$ (4.25 *vs.* 6.16 D).

The situation for $[mAT]^+$ is very different, the attempts to optimize proton-transferred structures of $[mAT]^+$ are all converged to the original $[mAT]^+$ base pair, although similar enhanced positive charges on hydrogen atoms of mA^+ has been observed. This suggests that adenine N6 is a better proton acceptor than thymine O4.

3.3 Deprotonation of $[mGC]^+$

The deprotonation of all active sites on $[mGC]^+$ gives nine deprotonated structures. They are mG(N1)C, mG(N2a)C, mG(N2b)C, mG(C8)C, mGC(N1), mGC(N4a), mGC(N4b), mGC(C5) and mGC(C6), respectively. Interestingly, it is found that a barrier-free proton transfer (BFPT) from mG^+ N1 to cytosine N3 accompanies the removal of a proton form cytosine N4, C5 or C6 site, respectively. Nevertheless, no such proton transfer is observed along with the loss of the proton attached to cytosine N1.

3.3.1 Geometries and relative stabilities. Geometrical characters of the deprotonated structures are summarized in Table S1 (ESI†). The relative energies of the deprotonated structures are reported in Table 6. Several deprotonated structures of $[mGC]^+$ are presented in Fig. 2.

The removal of a proton on mG^+N1 site generates mG(N1)C. This causes cytosine slide downward relative to mG^+ in a plane and thus leaves two N···H–N H-bonds (Fig. 2). This result may be surprising because the neutral N–H···N H-bonds are considered to be weaker than the neutral O–H···O–H-bonds. This may be due to the extended conjugation of the rings. This conclusion is supported by the fact that both the N–C bonds adjacent to the N1 center have been shortened greatly after deprotonation.

Table 6 Relative energies, dissociation energies (D_e) of the deprotonated structures derived from $[mGC]^+$ and GPAs for $[mGC]^+$

	ΔE/kcal mol^{-1}	GPA/eV	D_e/kcal mol^{-1}
mG(C8)C	0	12.05	24.34
mG(N1)C[a]	0.042	12.05	16.28
mGC(N4b)	2.76	12.17	16.99
mGC(N1)	8.83	12.43	100.00
mGC(N4a)	9.95	12.49	8.21
mG(N2b)C	14.49	12.68	12.70
mG(N2a)C	15.56	12.73	6.20
mGC(C6)	27.72	13.26	27.22
mGC(C5)	33.55	13.50	25.58

[a] GPA of mG(N1) is 262.87 kcal mol^{-1} (≈11.40 eV), taken from ref. 16, our result is about 11.30 eV.

For mG(N2a)C, removing the proton H2a results in the loss of an H-bond, leaving two H-bonds (N1–H1···N3 and N4–H4a···O6, Fig. 2). What's more, the planarity of the base pair is destroyed accompanying the loss of N2–H2a···O2 H-bond. The dihedral angles are −54.9 and −16.6° (Table S1, ESI†), respectively.

In the case of mG(N2b)C/mG(C8)C, the loss of a proton from mG^+ N2/C8 site, where it is not involved in H-bonding, slightly changes the geometry of the pair. The structure still remains planar and is characterized by three H-bonds. The O6···H4a bond length in which guanine acts as proton acceptor is shortened, whereas the other two (N3···H1 and O2···H2a) bonds in which guanine acts as proton donors are lengthened compared with $[mGC]^+$.

In mGC(N1), deprotonation from cytosine N1 site causes the planarity of the base pair disappear. Moreover, N3···H1 and O2···H2a H-bonds in which cytosine acts as H-bond acceptors are greatly shortened compared with those in $[mGC]^+$ (1.689 and 1.454 Å *vs.* 1.868 and 1.767 Å, respectively), especially the latter. Whereas O6···H4a in which cytosine acts as H-bond donor is slightly elongated

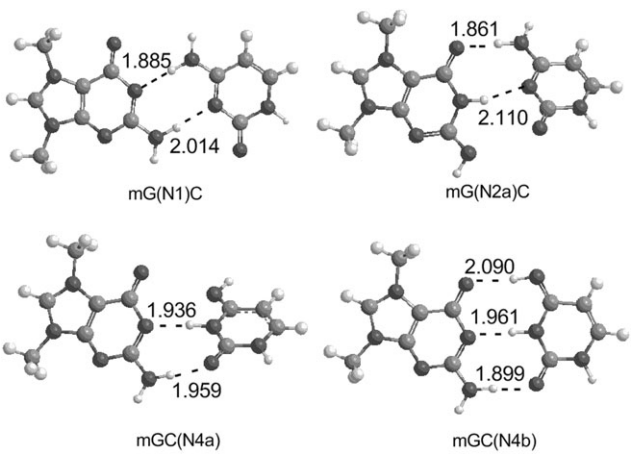

Fig. 2 Optimized structures of mG(N1)C, mG(N2a)C, mGC(N4a) and mGC(N4b).

(by 0.059 Å), no obvious changes are observed in H-bond angles. This could be explained when considering that the covalent binding of methyl carbonium to guanine increases its protondonor ability and the deprotonation from N1 site of cytosine simultaneously strengthens the proton-acceptor ability of cytosine. Both factors are positive for enhancing the H-bond strength.

Removing a proton from the N4 site of cytosine involving an H-bond gives mGC(N4a). The geometrical perturbations seen in Fig. 2 are large compared with $[mGC]^+$. A barrier-free proton transfer (H1) from the N1 site of mG^+ to N3 of cytosine is one of the notable changes observed. Another obvious change is that one of the three H-bonds involved in H-bonding is removed thus leaving two H-bonds (N1···N3 and N2···O2. But unlike the N1–H1···N3 H-bond before deprotonation, this H-bond becomes N1···H1–N3 after deprotonation as a result of BFPT mentioned above. The lengths of N1···H1 and O2···H2a are 1.930 and 1.959 Å, respectively. The distance of N1···N3 is 0.051 Å longer than that in $[mGC]^+$. Additionally, the planarity of the base pair is lost upon mGC(N4a) formation because of the large repulsion existing between the oxygen and nitrogen lone pairs during the deprotonation process. The dihedral angles of mGC(N4a) are −32.2 and −39.0° (Table S1, ESI†).

Upon removing the proton from the remaining active sites of cytosine, similar BFPT (from N1 site of guanine to N3 of cytosine) have been observed along with the formation of mGC(N4b) (Fig. 2), mGC(C5) and mGC(C6). O2···H2a H-bond in these three structures is elongated compared with those in $[mGC]^+$, while O6···H6a length is shortened.

The relative stabilities of the deprotonated $[mGC]^+$ are as follows: mG(C8)C ≈ mG(N1)C > mGC(N4b) > mGC(N1) > mG(N2b)C > mG(N2a)C > mGC(N4a) > mGC(C6) > mGC(C5) (Table 6). This order reflects the trends of deprotonation and should be closely associated with the GPAs.

3.3.2 GPAs. Table 6 and Fig. 3 show that C8 and N1 sites of guanine are the preferred regions for deprotonation, while C6 and C5 sites of cytosine are the two most unfavorable. It is known that the larger the value of GPA, the weaker the acidity is. Thus, protons on C8 and N1 sites of guanine are the most acidic of all active hydrogens. The least acidic hydrogens are those on C6 and C5 sites of cytosine. This relative acidic ordering of H-bound sites is somewhat inconsistent with that of the neutral GC reported by Lind *et al.*[8] They observed that the most acidic site of the neutral GC is the N1 site of cytosine (with GPA of 14.66 eV) and the least acidic one is C8 site of guanine. However, in our findings, N1 site of cytosine is the fourth acidic site, while both C8 and N1 sites of mG^+ are the first acidic sites among all H-bound sites of $[mGC]^+$. In view of the present result and also by comparison with the result reported by Lind *et al.*, GPA of N1 site on cytosine of the neutral GC was reproduced by us at the B3LYP/6-311++G**//B3LYP /6-31+G* level of theory. The result shows that GPA of N1–H on cytosine of the neutral GC is 14.65 eV, which is very close to 14.66 eV calculated by Lind *et al.*,[8] also indicating that all of these results are comparable. Thus, the comparisons of GPAs of $[mGC]^+$ in our research with those of the neutral GC reveal that the acidities of all

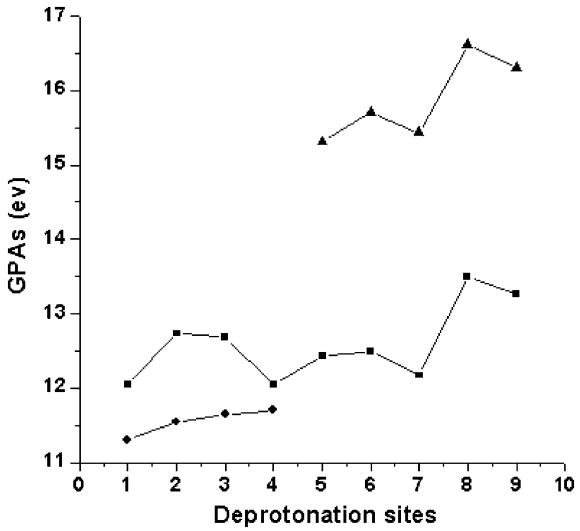

Fig. 3 Comparison of gas-phase acidity of all H-bound sites on $[mGC]^+$ with those of the isolated bases mG^+ and cytosine. Digits 1–9 on X-coordinates denotes the deprotonation sites guanine N1, N2a, N2b and C8, and cytosine N1, N4a, N4b, C5 and C6, respectively. GPA of mG(N1) in our computation is 11.40 eV, while that in ref. 16 is 11.30 eV. (■): GPAs of $[mGC]^+$; (●) and (▲): GPAs of the isolated mG^+ and cytosine, respectively.

H-bound sites are enhanced compared with those of the corresponding site of the neutral GC. The enhancement in acidity may mainly originate from the induction caused by guanine N7-methyl carbonium. As shown in Table 1, the total charges on guanine and cytosine moieties become more positive after methylation and it is thus not surprising that hydrogens on guanine and cytosine become more acidic. Additionally, in $[mGC]^+$, protons on guanine become less acidic, but protons on cytosine become more acidic than the corresponding proton in the isolated monomer, mainly because of the shifts of electron densities in the interbases. These changes of relative acidities can be seen from Fig. 3.

3.3.3 Dissociation energies. The dissociation scheme of several deprotonated structures of $[mGC]^+$ is displayed in Scheme 1. The corresponding dissociation energies are reported in Table 6. Scheme 2 reveals that mG(−H^+)C and mGC(N1) are dissociated into a deprotonated and a normal base. However, the dissociation of the other mGC(−H^+) except mGC(N1) actually gives mG(N1) and N3-protonated cytosine (−H^+) (namely, N3-protonated C(N4a), N3-protonated C(N4b), N3-protonated C(C5) and N3-protonated C(C6), respectively). Here, N3-protonated C(N4a) and N3-protonated C(N4b) are two imino forms of cytosine with the N4–H4b *trans* or *cis* to N3–H3 (denoted by *trans*-C* and *cis*-C*, respectively). This means that the dissociation of mGC(N4a)/mGC(N4b) generates mG(N1) and *trans*-C*/mG(N1) and *cis*-C*.

Among all deprotonated $[mGC]^+$, only mGC(N1) possesses a zwitterionic structure (0.748 e for mG^+ and −0.748 e for C(N1)) characterized by strong electrostatic attraction besides H-bond interactions between the two moieties. It is thus not surprising that the largest dissociation energy for mGC(N1) was predicted (100.00 kcal mol^{-1}, Table 6). This value is much

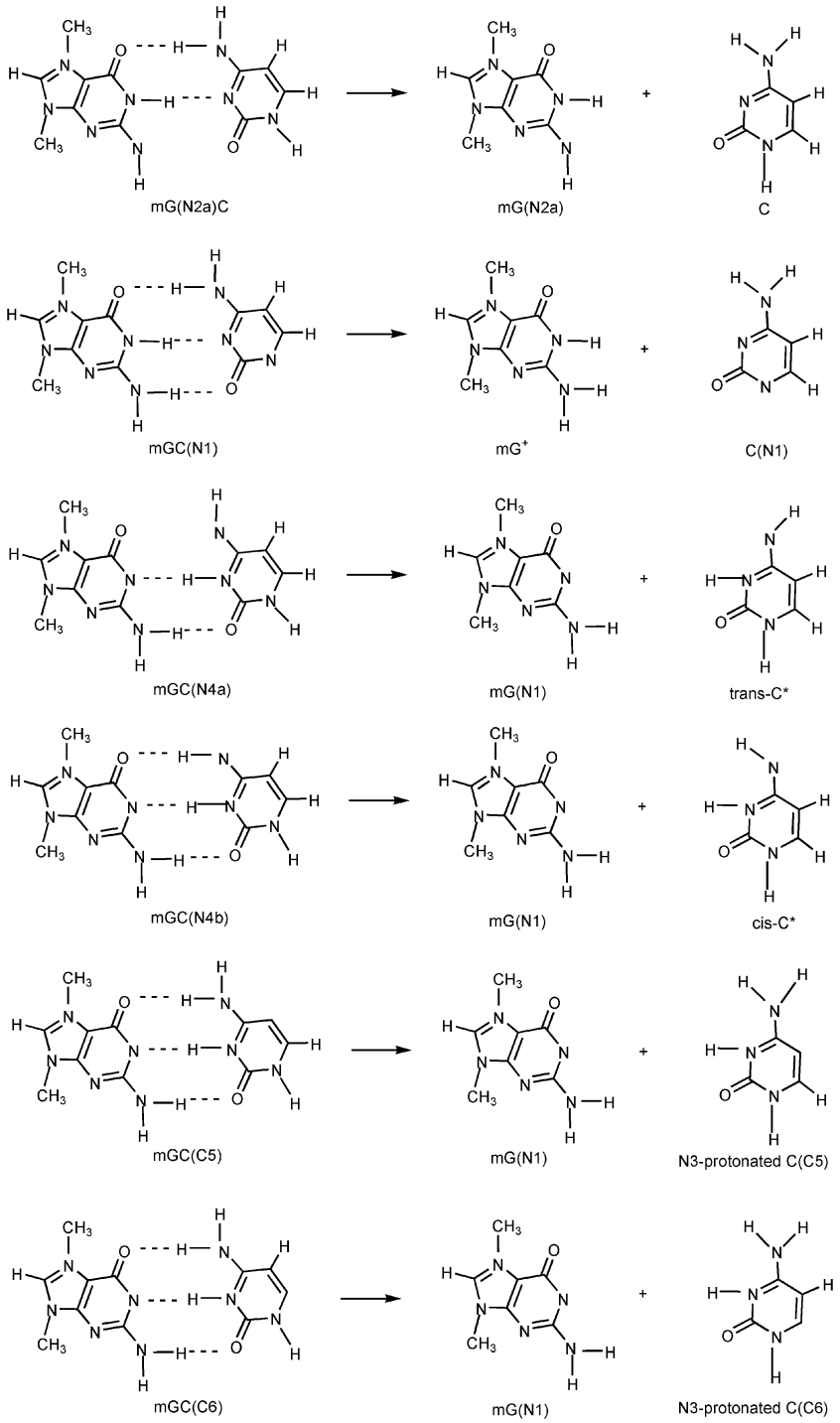

Scheme 1 The dissociation schemes for mG(N2a)C, mGC(N1), mGC(N4a), mGC(N4b), mGC(C5) and mGC(C6).

higher than that of $[mGC]^+$ or the neutral GC base pairs. The dissociation energies of the next three are slightly higher or comparable to that of the neutral GC (24.67 kcal mol^{-1}), but lower than that of $[mGC]^+$ (Table 6, mGC(C6), mGC(C5) and mG(C8)C). The remaining five deprotonated structures with the low dissociation energies are easily dissociated into their component bases. Among these five structures, it is interesting that the dissociation of mGC(N4a) and mGC(N4b) would generate two imino forms of cytosine—*trans*-C* and *cis*-C*. Thus, it can be deduced that a significant number of imino/enol tautomers could be formed in this way. Previous studies have hypothesized a modified tautomeric mechanism in which they suggest that the rare tautomers might be formed in the template *via* the concerted double proton transfer in the interbase H-bonds in DNA and thereby does not require the presence of the free rare tautomers in solution.[44,45] Our results may provide the theoretical support for this mechanism.

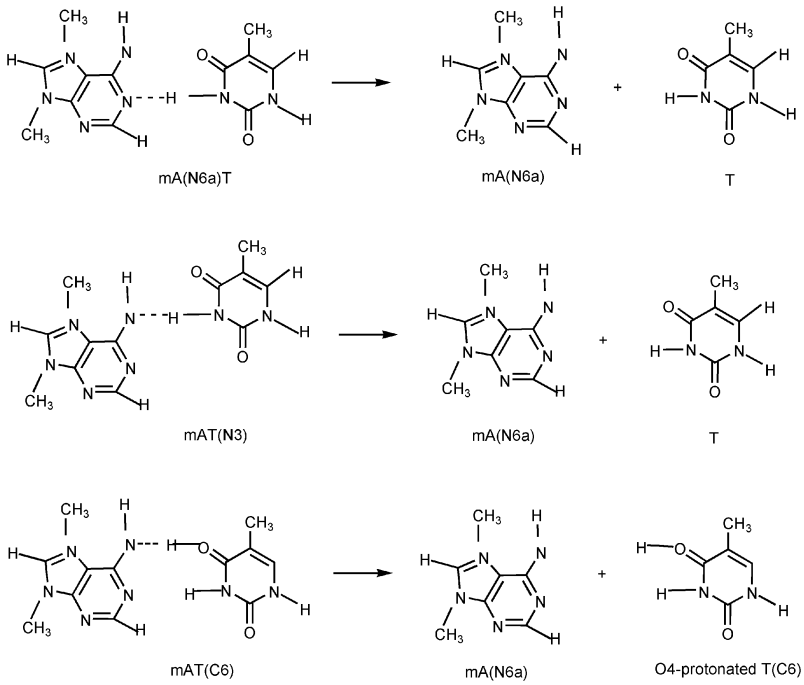

Scheme 2 The dissociation schemes for mA(N6a)T, mAT(N3) and mAT(C6).

3.4 Deprotonation of $[mAT]^+$

Seven deprotonated structures derived from $[mAT]^+$ have been obtained. They are mA(C2)T, mA(N6a)T, mA(N6b)T, mA(C8)T, mAT(N1), mAT(N3) and mAT(C6), respectively. Table S2, ESI† provides the details of the geometrical parameters of the deprotonated structures. The GPAs and the dissociation energies of the deprotonated $[mAT]^+$ are reported in Table 7. Structures [mA(N6a)T, mAT(C6) and mAT(N3)] with the great changes in geometries are shown in Fig. 4. In general, deprotonation of $[mAT]^+$ has the similar characteristics to that of $[mGC]^+$, such as the most preferred deprotonation site, the most stable deprotonated base pair and BFPT from purine to pyrimidine accompanying deprotonation from pyrimidine, except for the N1 site. Similarly, the acidities of all H-bound sites of $[mAT]^+$ are weaker than the corresponding sites of the isolated mA^+ and stronger than those of the isolated thymine (Fig. 5).

For $[mAT]^+$, the most preferred deprotonation region of all active sites is also the purine (mA^+) C8 site. The energy required for deprotonation from this region is about 11.53 eV (Table 7). mA(N6b)T is the second preferred one to be obtained. The most unfavorable deprotonation region is the mA^+ C2 site with the energy required of ~14.21 eV. This structure exhibits great deviation from the planarity with two dihedral angles predicted to be 33.5 and 20.1°, respectively. All of the three deprotonated structures are characterized by two H-bonds with N1···H3 bond being shortened and the other one being elongated.

Removal of a proton from the pyrimidine N1 site generates the most stable deprotonated base pair mAT(N1). Like the formation of mGC(N1), no spontaneous proton transfer is observed. In addition, it also possesses a zwitterionic structure characterized by large dipole moment. Thus it is natural that this structure has the largest dissociation energies among all deprotonated $[mAT]^+$ (~65.49 kcal mol^{-1}, Table 7). As anticipated, the removal of a proton from the N1 site of cytosine dramatically shortens the O4···H6a H-bond and slightly lengthens the N1···H3 bond.

Table 7 Relative energies (ΔE), GPAs and dissociation energies (D_e) of the deprotonated structures derived from $[mAT]^+$

	ΔE/kcal mol^{-1}	GPA/eV	D_e/kcal mol^{-1}
mA(C8)T	0	11.53	12.62
mA(N6b)T	4.83	11.87	9.54
mAT(N3)	13.61	12.13	11.98
mA(N6a)T	17.76	12.30	7.62
mAT(N1)	26.88	12.70	65.49
mAT(C6)	53.42	13.85	30.62
mA(C2)T	61.74	14.21	12.58

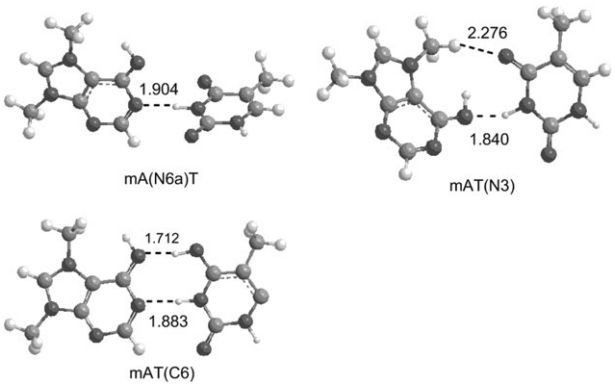

Fig. 4 Optimized structures of mA(N6a)T, mAT(N3) and mAT(C6).

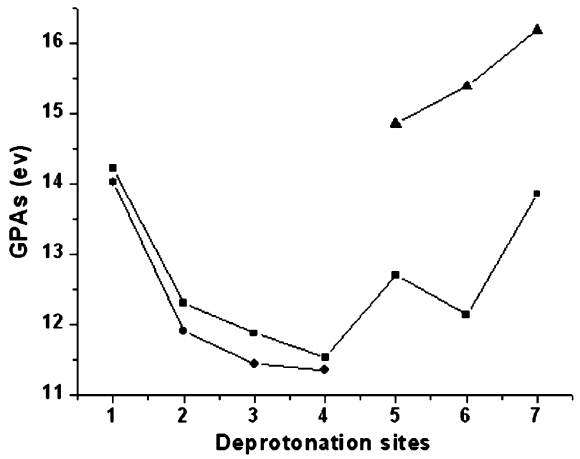

Fig. 5 Comparison of gas-phase acidity of all H-bound sites on $[mAT]^+$ with those of the isolated bases mA^+ and thymine. Digits 1–7 on X-coordinates denotes deprotonation sites adenine C2, N6a, N6b and C8; and thymine N1, N3 and C6, respectively. (■): GPAs of $[mAT]^+$; (●) and (▲): GPAs of the isolated mA^+ and thymine, respectively.

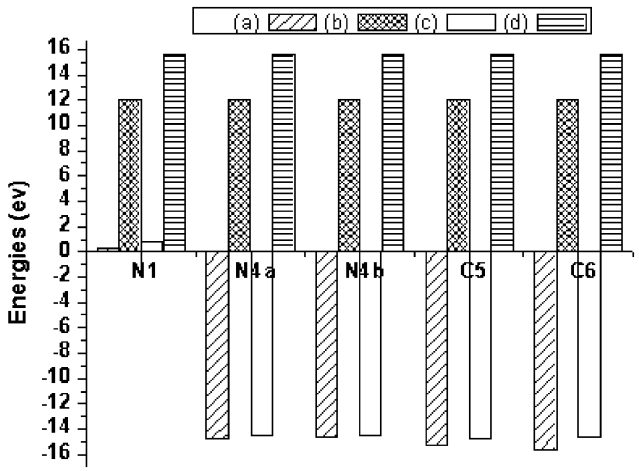

Fig. 6 Comparisons of the deprotonation energy of mG(N1)C (b) with N3-proton affinities of C(N1), C(N4a), C(N4b), C(C5) and C(C6) (a) as well as the deprotonation energy of mG(N2a)C (d) with O2-proton affinities of C(N1), C(N4a), C(N4b), C(C5) and C(C6) (c).

However, removing a proton involving H-bonds or from regions on pyrimidine leads to great changes on geometries (Fig. 4). For mA(N6a)T, it is generated by the removal of one of the protons (H6a) attached to N6 site of adenine. This causes the loss of one H-bond and induces the monomers to rotate away from each other to avoid the large repulsion of two lone pairs between mA^+ N6 and thymine O4, and thereby destroys the planarity of the pair. This structure has the lowest dissociation energy, indicating that deprotonation form this site would greatly change the structural and energetic characteristics and consequent DNA strand.

In the case of mAT(N3), the planarity is also lost along with the loss of N1···H H-bond (with two dihedral angles between two bases of 34.7 and 11.4°, respectively). At the same time, thymine slides upward relative to mA^+ to avoid the repulsion between two nitrogen lone pairs, and H6a on N6 spontaneously transfers to N3 of thymine. Thus, the resulting structure is characterized by a strong H-bond N6···H6a–N3 with H-bond length 1.840 Å. Additionally, there is a weak interaction between O4 of thymine and N7-methyl hydrogen atom of mA^+ with bond length ~2.276 Å, which may provide additional stabilization energy for the deprotonated structure. As expected, the dissociation energy of this deprotonated structure is comparable to that of the canonical AT pair (11.98 *vs.* 11.96 kcal mol^{-1}), despite losing one H-bond and having a nonplanar structure.

For mAT(C6), spontaneous proton transfer from N6 of mA^+ to O4 of thymine is observed along with the mAT(C6) formation. This structure remains planar and is characterized by two H-bonds: N6···H6a and N1···H3. The sum of two H-bond lengths of mAT(C6) are shorter than that of $[mAT]^+$.

In summary, the relative deprotonation order is as follows: mA(C8)T > mA(N6b)T > mAT(N3) > mA(N6a)T > mAT(N1) > mAT(C6) > mA(C2)T, while the dissociation energies of the deprotonated base pairs follows the order: mAT(N1) > mAT(C6) > mA(C8)T > mA(C2)T > mAT(N3) > mA(N6b)T > mA(N6a)T (Table 7).

3.5 N3-/O2-Protonation of C(−H^+)

As mentioned above, a barrier-free proton transfer (BFPT) from guanine N1 to cytosine N3 accompanies deprotonation from the N4, C5 or C6 site of cytosine. It is surprising that this phenomenon has not been observed when a proton is removed from cytosine N1 site of $[mGC]^+$ or a proton is removed from all H-bound sites on cytosine of the neutral GC. On the other hand, no BFPT from guanine N2 site to cytosine O2 site is found, although it has been reported that the gas-phase proton affinities of O2 and N3 sites of cytosine differ by less than 1 kcal mol^{-1}.[9]

To further explore the reason of BFPT of H1 on guanine, the N3-proton affinities of C(−H^+) and the energy requirement for deprotonation at guanine N1 site of $[mGC]^+$ are compared. Fig. 6 shows that N3-proton affinities of C(N4a), C(N4b), C(C5) and C(C6), ranging from −14.63 to −15.63 eV, are higher (absolute value) than the energy requirement for deprotonation from the N1 site on mG^+ (GPA of deprotonation at guanine N1 site of $[mGC]^+$ is 12.05 eV as shown in Table 6). Therefore, proton-transfer reaction between two sites is thermodynamically favorable and thereby H1 spontaneously transfers to cytosine N3. However, the N3-proton affinity of C(N1) are positive (0.31 eV), indicating that the N3-protonated reaction of C(N1) is non-spontaneous. Thus, removing a proton from N1 site of cytosine would not promote the formation of N3-protonated C(N1). This may be because C(N1) is resonance-stabilized by the carbonyl group on the one hand and C=C double bond on the other and thus decreases its ability to accept a proton.

To analyze the possibility of BFPT of H2a on guanine accompanying the deprotonation from sites on cytosine of $[mGC]^+$, the O2-proton affinity of C(−H^+) and the energy needed for deprotonation at guanine N2 site of $[mGC]^+$ are also calculated. O2-proton affinities of C(N1), C(N4a), C(N4b), C(C5) and C(C6) are 0.79, −14.62, −14.73, −14.51 and −14.47 eV, respectively. These proton affinities are smaller (absolute value) than the energy needed for removing a proton from N2a site of mG^+ (~15.56 eV). That is, proton-transfer

reaction from N2 of guanine to O2 of cytosine is thermodynamically unfavorable and thereby no BFPT from guanine N2 site to cytosine O2 site would be observed. This is supported by the fact that H2a does not transfer to O2 site on cytosine when deprotonation at sites on cytosine of $[mGC]^+$ as described above.

4 Concluding remarks

In the present paper, we successfully optimized the structures of $[mGC]^+$ and $[mAT]^+$ as well as deprotonated structures derived from $[mGC]^+$ and $[mAT]^+$ base pairs. Moreover, the transition state has been located for the proton-transfer process in the $[mGC]^+$ pair. Several conclusions can be drawn:

(1) The covalent binding of methyl carbonium to guanine/adenine N7 strengthens the H-bond in which purine acts as proton donor and weakens the H-bond in which purine acts as proton acceptor and thus enhances the stability of the GC/AT base pair. NBO analyses are in good agreement with these changes.

(2) Methyl carbonium binding to the guanine N7 site promotes proton transfer from the guanine N1 site to the cytosine N3 site. The structure of the transition state for the proton-transfer process is out-of-plane. The activation energy for the proton transfer of the $[mGC]^+$ cation is 6.93 kcal mol^{-1}, while the reverse activation energy is 0.9 kcal mol^{-1}. However, if taking ZVPE into consideration, the reverse activation energy becomes negative. So $[mGC]^+$ is the predominating species in the gas phase. In the case of the $[mAT]^+$ base pair, no such proton-transferred structure is obtained in $[mAT]^+$, whether single or double proton-transferred structure.

(3) As for the deprotonation of $[mGC]^+$ and $[mAT]^+$, the most preferred deprotonation sites are the guanine C8 and N1 sites and adenine C8 site, respectively. Of all deprotonated structures derived from $[mGC]^+/[mAT]^+$, the removal of a proton from the pyrimidine N1 site generates the most stable deprotonated base pair, since this pair has a zwitterionic structure.

(4) Additionally, it is interesting that deprotonation from pyrimidine, except the pyrimidine N1 site which is attached to deoxyribose, is accompanied by a barrier-free proton transfer (BFPT) from purine to pyrimidine. However, deprotonation from the pyrimidine N1 site would not promote such proton transfer. BFPT from guanine N1 to cytosine N3 results in two rare tautomers of cytosine (*trans*-C* and *cis*-C*), indicating that a significant number of the rare tautomers of cytosine might be formed in such a way.

(5) The calculated N3-proton affinities and O2-proton affinities of C(N4a), C(N4b), C(C5) and C(C6) reveal that proton-transfer reaction from guanine N1 site to cytosine N3 site is thermodynamically favorable, while that from guanine N2 site to cytosine O2 site is thermodynamically unfavorable. So only BFPT from guanine N1 to cytosine N3 site is observed.

Acknowledgements

This work is supported by NSFC (20573063, 20633060) to Y. B., NIH (Grant No. GM62790) to R. I. C., NCET and shandong-NSF (Z2003B01) to Y. B. Support to Y. B. from Virt Lab Comput Chem of CNIC and Supercomputing Center of CNIC-CAS are also acknowledged. A part of calculations were performed on the CBM and the MCBILIN clusters at Michigan State University, and HPCC at Shandong University. The author (Y. B.) also thanks Prof. Yi Hu for his help in calculations.

References

1 A. M. Lamsabhi, M. Alcamí, O. Mó and M. Yáñez, *J. Phys. Chem. A*, 2006, **110**, 1943–1950.
2 I. A. Topol, S. K. Burt, M. Toscano and N. J. Russo, *Mol. Struct. (THEOCHEM)*, 1998, **430**, 41–49.
3 A. G. Harrison, *Mass Spectrom. Rev.*, 1997, **16**, 201.
4 C. Munôz-Caro, A. Ninô, M. L. Senent, J. M. Leal and S. Ibeas, *J. Org. Chem.*, 2000, **65**, 405.
5 A. A. Bliznyuk, H. F. Schaefer and I. J. Amster, *J. Am. Chem. Soc.*, 1993, **115**, 5149.
6 O. N. Ventura, J. B. Rama, L. Turi and J. J. Dannenberg, *J. Am. Chem. Soc.*, 1993, **115**, 5754.
7 P. P. Bera and H. F. Schaefer, *Proc. Natl. Acad. Sci. USA*, 2005, **102**, 6698.
8 M. C. Lind, P. P. Bera, N. A. Richardson, S. E. Wheeler and H. F. Schaefer, *Proc. Natl. Acad. Sci. USA*, 2006, **103**, 7554.
9 J. Florián and J. Leszczyñski, *J. Am. Chem. Soc.*, 1996, **118**, 3010.
10 (*a*) R. Purrello, M. Molina, Y. Wang, G. Smulevich, J. Fossella, J. R. Fresco and T. G. Spiro, *J. Am. Chem. Soc.*, 1993, **115**, 760; (*b*) F. A. Evangelista, A. Paul and H. F. Schaefer, *J. Phys. Chem. A*, 2004, **108**, 3565; (*c*) N. Russo, M. Toscano, A. Grand and F. Jolibois, *J. Comput. Chem.*, 1998, **19**, 989; (*d*) I. A. Topol, S. K. Burt, N. Russo and M. Toscano, *J. Am. Soc. Mass Spectrom.*, 1999, **10**, 318; (*e*) P. Li, Y. X. Bu, H. Q. Ai and Z. H. Cao, *J. Phys. Chem. A*, 2004, **108**, 4069.
11 B. Song, J. Zhao, R. Griesser, C. Meiser, H. Sigel and B. Lippert, *Chem. Eur. J.*, 1999, **5**, 2374.
12 B. Lippert, *Coord. Chem. Rev.*, 2000, **200–202**, 487–516.
13 J. V. Burda, J. Sponer and P. Hobza, *J. Phys. Chem.*, 1996, **100**, 7250.
14 J. K. Snyder, *L. M. Stock J. Org. Chem.*, 1980, **45**, 1990.
15 R. Saffhill, G. P. Margison and P. Oconnor, *Biochim. Biophys. Acta*, 1985, **823**, 111.
16 J. V. Burda, J. Sponer J. Hrabakova, M. Zeizinger and J. Leszczynski, *J. Phys. Chem. B*, 2003, **107**, 5349.
17 S. Boiteux and J. Laval, *Biochem. Biophys. Res. Commun.*, 1983, **110**, 552.
18 T. R. Oconnor, S. Boiteux and J. Laval, *Nucleic Acids Res.*, 1988, **16**, 5879.
19 B. Tudek, S. Boiteux and J. Laval, *Nucleic Acids Res.*, 1992, **20**, 3079.
20 K. O. Roland, S. E. Freisinger and B. Lippert, *J. Biol. Inorg. Chem.*, 2000, **5**, 287.
21 L. J. Marnett and P. C. Burcham, *Chem. Res. Toxicol.*, 1993, **6**, 771.
22 T. Lindahl, B. Sedgwick, M. Sekiguchi and Y. Nakabeppu, *Annu. Rev. Biochem.*, 1988, **57**, 133.
23 D. T. Beranek, C. C. Weis and D. H. Swenson, *Carcinogenesis.*, 1980, **1**, 595–606.
24 P. D. Lawley, *Chemical Carcinogenesis; ACS Monograph 182*, ed. C. E. Searle, American Chemical Society, Washington, DC, 1984, **vol. 1**, p. 325.
25 G. K. Forde, A. E. Forde, G. Hill, A. Ford, A. Nazario and J. Leszczynski, *J. Phys. Chem. B*, 2006, **110**, 15564.
26 K. S. Ekanayake and R. L. Pierrer, *J. Comput. Chem.*, 2006, **27**, 277, and references therein.
27 C. F. Guerra, T. Wijst and F. M. Bickelhaupt, *Chem. Eur. J.*, 2006, **12**, 3032–3042.
28 C. F. Guerra, F. M. Bickelhaupt, J. G. Snijders and E. Baerends, *Chem. Eur. J.*, 1999, **5**, 3581–3594.
29 J. Bertran, A. Oliva, L. Rodrıguez-Santiago and M. Sodupe, *J. Am. Chem. Soc.*, 1998, **120**, 8159–8167.

30 J. Sponer, M. Sabat, L. Gorb, J. Leszczynski, B. Lippert and P. Hobza, *J. Phys. Chem. B*, 2000, **104**, 7535–7544.
31 L. X. Sun and Y. X. Bu, *J. Phys. Chem. B*, 2005, **109**, 593.
32 (*a*) M. Noguera, J. Bertran and M. Sodupe, *J. Phys. Chem. A*, 2004, **108**, 333–341; (*b*) J. V. Burda, J. Sÿponer, J. Leszczynski and P. Hobza, *J. Phys. Chem. B*, 1997, **101**, 9670–9677; (*c*) J. Sÿponer, J. V. Burda, M. Sabat, J. Leszczynski and P. Hobza, *J. Phys. Chem. A*, 1998, **102**, 5951–5957.
33 (*a*) M. Brandl, M. Meyer and J. Sühnel, *J. Am. Chem. Soc.*, 1999, **121**, 2605; (*b*) M. Meyer, M. Brandl and J. Sühnel, *J. Phys. Chem. A*, 2001, **105**, 8223.
34 (*a*) A. D. Becke, *J. Chem. Phys.*, 1993, **98**, 5648; (*b*) C. Lee, W. Yang and R. G. Parr, *Phys. Rev. B*, 1988, **37**, 785.
35 P. J. Stephens, F. J. Devlin, C. F. Chabalowski and M. J. Frisch, *J. Phys. Chem.*, 1994, **98**, 11623.
36 M. J. Frisch, G. W. Trucks, H. B. Schlegel, G. E. Scuseria, M. A. Robb, J. R. Cheeseman, V. G. Zakrzewski, J. A. Montgomery, Jr, R. E. Stratmann, J. C. Burant, S. Dapprich, J. M. Millam, A. D. Daniels, K. N. Kudin, M. C. Strain, O. Farkas, J. Tomasi, V. Barone, M. Cossi, R. Cammi, B. Mennucci, C. Pomelli, C. Adamo, S. Clifford, J. Ochterski, G. A. Petersson, P. Y. Ayala, Q. Cui, K. Morokuma, D. K. Malick, A. D. Rabuck, K. Raghavachari, J. B. Foresman, J. Cioslowski, J. V. Ortiz, B. B. Stefanov, G. Liu, A. Liashenko, P. Piskorz, I. Komaromi, R. Gomperts, R. L. Martin, D. J. Fox, T. Keith, M. A. Al-Laham, C. Y. Peng, A. Nanayakkara, C. Gonzalez, M. Challacombe, P. M. W. Gill, B. G. Johnson, W. Chen, M. W. Wong, J. L. Andres, M. Head-Gordon, E. S. Replogle and J. A. Pople, *GAUSSIAN 98*, Gaussian Inc., Pittsburgh, PA, 1998.
37 (*a*) J. M. Galbraith and H. F. Schaefer, *J. Chem. Phys.*, 1996, **105**, 862; (*b*) N. Roesch and S. B. Trickey, *J. Chem. Phys.*, 1997, **106**, 8940.
38 S. S. Wesolowski, M. L. Leininger, P. N. Pentchew and H. F. Schaefer, *J. Am. Chem. Soc.*, 2001, **123**, 4023.
39 J. C. Rienstra-Kiracofe, C. J. Barden, S. T. Brown and H. F. Schaefer, *J. Phys. Chem. A*, 2001, **105**, 524.
40 S. F. Boys and F. Bernardi, *Mol. Phys.*, 1970, **19**, 553.
41 (*a*) A. Reed, L. A. Curtiss and F. Weinhold, *Chem. Rev.*, 1988, **88**, 899; (*b*) A. Reed, F. Weinhold, L. A. Curtiss and D. Pochatko, *J. Chem. Phys.*, 1986, **84**, 5687; (*c*) A. Reed and F. Weinhold, *J. Chem. Phys.*, 1985, **83**, 1736; (*d*) A. Reed, R. B. Weinstock and F. Weinhold, *J. Chem. Phys.*, 1985, **83**, 735.
42 X. Li, Z. Cai and M. D. Sevilla, *J. Phys. Chem. B*, 2001, **105**, 10115.
43 (*a*) A. O. Colson, B. Besler and M. D. Sevilla, *J. Phys. Chem.*, 1992, **96**, 9787; (*b*) A. O. Colson, B. Besler, D. M. Close and M. D. Sevilla, *J. Phys. Chem.*, 1992, **96**, 661.
44 P. O. Löwdin, *Adv. Quantum Chem.*, 1965, **2**, 213.
45 (*a*) P. O. Löwdin, in *Electronic Aspects of Biochemistry*, ed. B. Pullman, Academic Press, New York, 1964, p. 167; (*b*) P. O. Löwdin, *Mutation Res.*, 1965, **2**, 218.

